Journal of Hydrology 630 (2024) 130677

Contents lists available at ScienceDirect

Journal of Hydrology

journal homepage: www.elsevier.com/locate/jhydrol

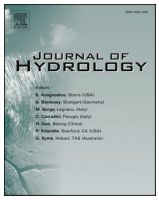

Research papers

Dynamic hydrological niche segregation: How plants compete for water in a semi-arid ecosystem

Ying Zhao [a,b,e], Li Wang [a,b,*], Kwok P. Chun [c], Alan D. Ziegler [d], Jaivime Evaristo [e,*]

[a] College of Natural Resources and Environment, Northwest A&F University, Yangling, Shaanxi, China
[b] Institute of Soil and Water Conservation, Chinese Academy of Sciences and the Ministry of Water Resources, Yangling, Shaanxi, China
[c] Department of Geography and Environmental Management, University of the West of England, Bristol, UK
[d] Faculty of Fisheries Technology and Aquatic Resources, Maejo University, Chiang Mai, Thailand
[e] Copernicus Institute of Sustainable Development, Utrecht University, Utrecht, The Netherlands

ARTICLE INFO

Keywords:
Hydrological niche segregation
Plant water uptake
Loess Plateau
Stable isotopes
nicheROVER

ABSTRACT

Hydrological niche segregation (HNS), specifically the variation in root water uptake depth among coexisting species, is an understudied area of research. This is especially the case in semi-arid ecosystems, such as China's Loess Plateau (CLP), where seasonal aridity necessitates adaptive water use strategies among plant species. In this study, we conducted a two-year investigation to understand the water sources and intrinsic water use efficiency (WUEi) of four coexisting plant species: *Populus simonii* (tree), *Caragana korshinskii* and *Salix psammophila* (shrubs), and *Artemisia ordosica* (semi-shrub). We analyzed the isotopic compositions of xylem and soil water (δ^2H and $\delta^{18}O$) and leaf $\delta^{13}C$ to identify the water sources and WUEi, respectively, of each species. We then used the nicheROVER model to quantify HNS based on the variations in xylem water δ^2H and $\delta^{18}O$. Our results show that the four co-existing species occupied distinct positions on a hydrological niche axis, delineated by their respective water sources and disparate WUEi. The tree *P. simonii* exhibited a preference for deep soil water and demonstrated a high WUEi. Both shrubs, *S. psammophila* and *C. korshinskii*, utilized intermediate and deep soil water, respectively, and with comparable WUEi. Conversely, the semi-shrub *A. ordosica* relied on shallow soil water and displayed a low WUEi. These differences in water sources and WUEi led to HNS between *A. ordosica* and the other three species in a relatively wet year. However, in a relatively dry year, HNS between *A. ordosica* and the other three species contracted and WUEi increased as species increased the use of deep soil water. Overall, these results demonstrate that HNS is a dynamic phenomenon that varies on at least an annual basis. It expands and contracts as plants regulate their water uptake and loss in response to changing soil moisture conditions.

1. Introduction

Water is the most limiting resource for plant survival and growth in arid and semi-arid ecosystems. Coexisting plant species usually adopt diverse water use strategies (e.g., root biomass adjustment, shift in root water uptake depth, stomatal regulation) to compete for or apportion this limited resource within mixed communities (Granda et al., 2022; Kulmatiski et al., 2020b; Rodríguez-Robles et al., 2020). Silvertown et al. (2015) introduced the concept of hydrological niche segregation (HNS) regarding the apportionment of soil water resources. HNS comprises three aspects: (a) partitioning of space along fine-scale moisture gradients; (b) partitioning of water as a resource; and/or (c) partitioning of recruitment opportunities due to species specializing in certain patterns of temporal water supply or storage variance.

The HNS concept has found applications in a wide range of environments such as wet meadows, coastal dune slacks, tropical rainforests, savannas, and Mediterranean climates (Araya et al., 2011; Bartelheimer et al., 2010; Camarero et al., 2018; Case et al., 2020; Dwyer et al., 2021; Holdo and Nippert, 2023; Kulmatiski et al., 2020a; Matos et al., 2022; Wu et al., 2022a). A commonality in these studies is that root distributions in the soil can cause variability in soil water resources available to different plants. Walter's two-layer hypothesis (1939) posits that trees and grasses coexist by exploiting different soil water depths: trees access deep soil water with their deep roots; meanwhile grasses, with their shallow roots, utilize near-surface soil water (Ward et al., 2013). A recent study on a savanna ecosystem corroborates this notion by

* Corresponding authors at: Institute of Soil and Water Conservation, Northwest A&F University, Yangling, Shaanxi, China (Li Wang).
E-mail addresses: wangli5208@nwsuaf.edu.cn (L. Wang), j.evaristo@uu.nl (J. Evaristo).

https://doi.org/10.1016/j.jhydrol.2024.130677
Received 8 September 2023; Received in revised form 23 November 2023; Accepted 30 November 2023
Available online 24 January 2024

demonstrating how the shallow roots of grasses promote rapid access to sufficient soil water, enabling constant grass cover, while the slightly deeper roots of trees access more water throughout the soil profile under most conditions (Kulmatiski and Beard, 2022).

HNS among coexisting species, influenced by differences in root distribution, is evident not only in spatially segregated deep and shallow water stores (sources for plants), but also may exhibit temporal segregation because of differences in soil water age. This segregation is known as "root-niche separation", which occurs in systems where deep-rooted vegetation uses the water stored from wet-season precipitation during the dry season, while more shallow-rooted species directly access dry-season precipitation if any (Ivanov et al., 2012). A global assessment comparing inverse modeling and isotope-based estimates suggested, similarly, that 19% of plant transpiration water relied on precipitation stored in deeper unsaturated soil, rocks and groundwater during past events; and 70 % relied on precipitation in the current month (Miguez-Macho and Fan, 2021).

Coexisting plant species not only maximize their access to limited soil water resources through the temporal and spatial segregation of hydrological niches, but they also respond to water resource shortages through their own physiological regulations (Illuminati et al., 2022; Rodríguez-Robles et al., 2020). Intrinsic water use efficiency (WUEi)—the amount of carbon fixed per unit of water consumed—inferred from $\delta^{13}C$ values of plant leaves or tree rings, has been used to indicate the ability of plants to adapt to and tolerate extended dry periods and droughts. Thus, the variable is an indicator of the differentiation of physiological traits among coexisting species under different water stress conditions (Angert et al., 2009; Araya et al., 2010). In one example, Moreno-Gutierrez et al. (2012) found that ten co-existing plant species in a Mediterranean ecosystem exhibited diverse stomatal regulation and water use strategies. Some were "opportunistic" with high stomatal conductance and low WUEi; others "conservative", having low stomatal conductance and high WUEi. The ecophysiological niche segregation was observable in leaf $\delta^{18}O$ and $\delta^{13}C$ data. Another study based on the comparison of tree-ring $\delta^{13}C$ and radial-growth rates of three tree species in two Mediterranean sites similarly found that species with contrasting hydrological niches showed divergent WUEi and growth rates (Camarero et al., 2018). Other studies have used root depth, access to light, and leaf hydrological traits to assess differences in physiological traits of co-existing species (Brum et al., 2017, 2019).

Overall, the spatio–temporal segregation of hydrological niche of coexisting species not only facilitates efficient soil water use, but also alters the expression of physiological traits. However, the physiological mechanisms and root water uptake of coexisting species, and how they function together to manage water stress, have not been fully investigated (Rodríguez-Robles et al., 2020). While much is known about the various strategies plants (especially trees and crops) use to avoid and tolerate water stress, such as anatomical alterations, physical acclimations, gene signaling, metabolic reactions, and rhizosphere interactions (Brunner et al., 2015; Daly et al., 2017; Kang et al., 2022), coordination of hydrological niches and drought tolerance strategies require further investigation.

In this study, we characterize the water use strategies and HNS of four coexisting plant species (*Populus simonii* (tree), *Caragana korshinskii* (shrub), *Salix psammophila* (shrub), and *Artemisia ordosica* (semi-shrub)) in a semi-arid ecosystem in China's Loess Plateau (CLP). In the study we combined traditional, isotopic, and modeling approaches to identify water sources, calculate WUEi and water stress, and investigate the degree of HNS occurring in two years, one relatively dry, the other relatively wet. We explore three hypotheses: (1) the four target plant species have distinct water uptake depths and WUEi; (2) there is clear HNS among the species; and (3) HNS is dynamic in response to changing soil moisture patterns on an annual scale, but likely dampened because of the limited water holding capacity of the sandy soil texture at the site.

2. Materials and methods

2.1. Study area

The study was conducted in the Liudaogou Catchment (38°47′–38°49′N, 110°21′–110°23′E), which is located on the southern edge of the Mu Us Sandy Land, in Shaanxi province of China (Fig. 1a). The catchment is part of the Grain for Green project, which was launched in 1999 to combat erosion on the CLP and sediment buildup in the Yellow River (Chen et al., 2015). The Liudaogou Catchment is about 6.89 km^2 and ranges in altitude from 1094 m to 1274 m. The regional climate is classified as semi-arid with cold winters, low annual rainfall and strong seasonal variations in moisture (Fu et al., 2017; Tsunekawa et al., 2014). The average annual precipitation is 464 ± 121 mm based on data from 2003 to 2019 (Zhao et al., 2022). Most of the annual precipitation, 70–80 %, falls from June to August, while winter snowfall (December–February) is only about 10 mm on average based on data from 2003 to 2019.

Surficial soil in the study area has evolved from loess material transported by strong storms from distant northwest locations throughout the Quaternary (Fu et al., 2017; Liu, 1985). The relief of the underlying parent material is relatively flat, but details are masked by the deposition of both ancient (Pleistocene) and contemporary eolian sands (Zhang et al., 1993). Our experimental plot was located in flat sandy areas and the soil texture is nearly all sand (USDA classification): the material in the 0–300 cm layer is composed of 95.7 % sand, 3.2 % silt, and 1.1 % clay (Fig. 1b). Relatively uniform particle composition greatly reduces the potential impact of spatial heterogeneity of soil water on this study.

Native plants are scarce at the site, except for a few surviving shrub species such as *Artemisia ordosica* Krasch, *Xanthoceras sorbifolium* Bunge, and *Ulmus macrocarpa* Hance (Yuan et al., 2017). Vegetation coverage has increased significantly due to the Three-North Shelter Forest and the Grain for Green programs (Lu et al., 2018). Common species used in the reforestation include *Populus simonii* Carr., *Salix matsudana* Koidz., *Salix psammophila*, and *Caragana korshinskii* Kom. Initial forestation activities mainly involved replanting forest species (Cao, 2008). These restored forests then evolved into tree-shrub complex ecosystems (Cao et al., 2010, 2011). Poplar trees (*P. simonii*) were planted in our study location about 40 years ago over an area of 40 ha. Over time, three understory species – Korshinsk pea (*C. korshinskii*), xerophytic shrub (*S. psammophila*), and a dwarf, sand-binding semi-shrub (*A. ordosica*) – have emerged due to seed dispersal by wind and birds (Fig. 1c).

In the study, we determined vegetation characteristics of the four species within a one-hectare (100 m × 100 m) survey plot (Fig. S1). Within the plot, we collected nine 20 × 20 m^2 tree quadrats, located at all locations of the diagonals of the one-hectare plot, and eighty-one 4 × 4 m^2 shrub sub-quadrats, located at all locations of the diagonals of the 400-m^2 tree quadrat (Kang et al., 2007). *A. ordosica* is the most abundant, with 3356 individuals per hectare. The densities of *P. simonii*, *C. korshinskii*, and *S. psammophila* are much lower, at 519, 494, and 301 individuals per hectare, respectively. *P. simonii* is the tallest of these species, with a mean height of about 5.2 m, while *C. korshinskii*, *S. psammophila*, and *A. ordosica* have mean heights of 1.4 m, 1.4 m, and 0.5 m, respectively (Table 1).

2.2. Meteorological data

Precipitation and air temperature (with 30-min resolution) data were obtained from a weather station located about 1500 m from the sampling plot. Precipitation was measured using TE525 tipping bucket rain gauges (Campbell Scientific Inc.), which has an accuracy of ± 1 percent. The air temperature was measured using HMP45D probes, which have ± 0.2 °C accuracy (Vaisala Inc.).

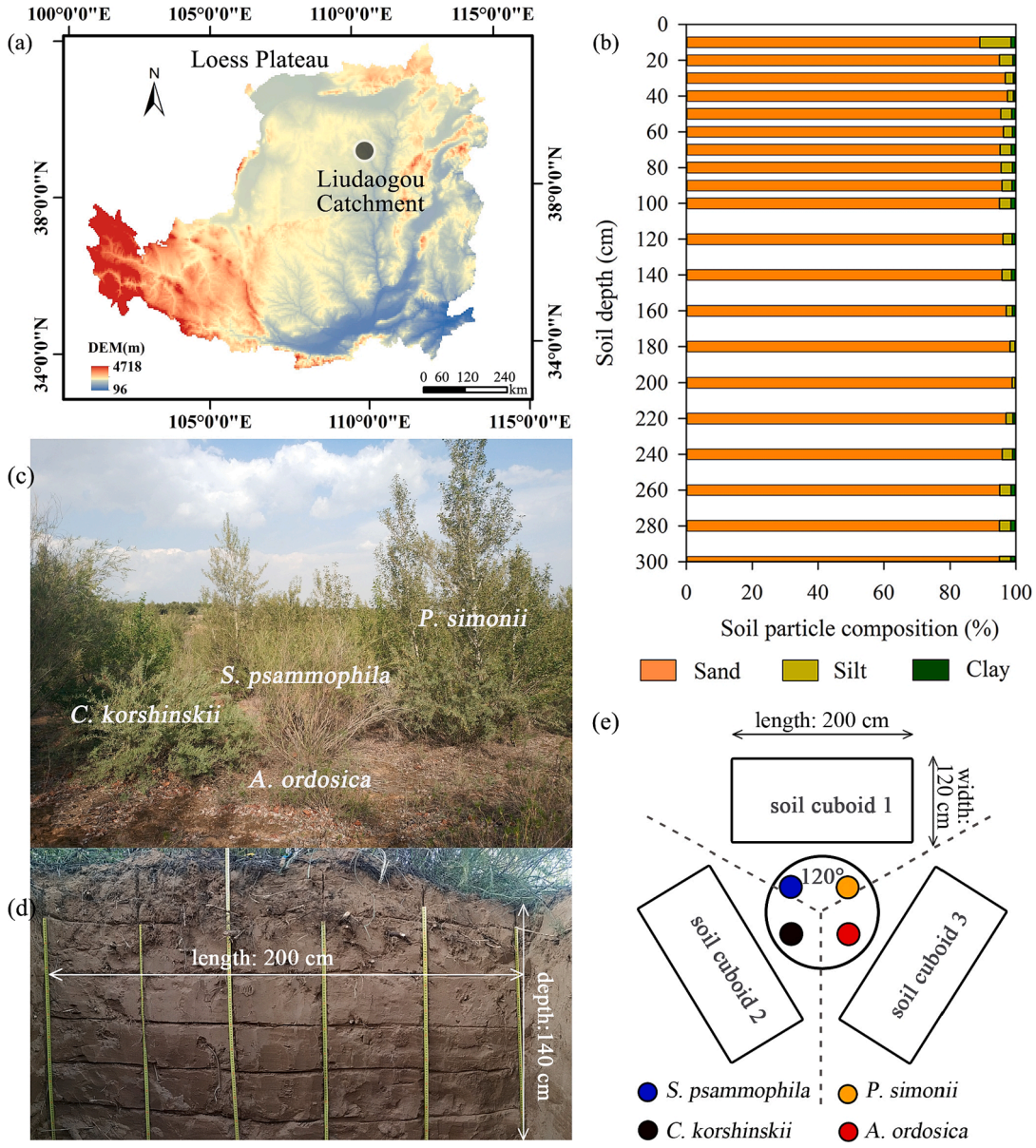

Fig. 1. Geographical location of the study area (a). Soil particle composition at 0–300 cm depths (b), photographs of four coexisting plant species (*P. simonii, S. psammophila, C. korshinskii* and *A. ordosica*) (c), and root excavations (not all depths are shown for clarity, d), and schematic of root excavations in our study area (e).

2.3. Classification of the relatively dry and the wet years

According to Tao et al. (2000) and Wang et al. (2016), we divided the relatively dry and wet years using precipitation and its standard deviation, as follows:

$$\text{The relatively wet year}: P_i > \overline{P} + 0.33\sigma \quad (1)$$

$$\text{The relatively dry year}: P_i < \overline{P} - 0.33\sigma \quad (2)$$

where P_i and $\overline{P}$ are the annual precipitation (mm) and the multi-year average precipitation (mm), respectively. σ is the standard deviation (mm).

In our study, $\overline{P}$ and σ are 464 mm and 121 mm, respectively, based on precipitation data from 2003 to 2019. During the two years of study, 2018–2019, precipitation was 708 mm and 424 mm, thus representing a relatively wet year and a relatively dry year, respectively.

2.4. Root excavations and measurements

In September 2019, we collected samples of fine roots (≤2 mm diameter) from four plant species (*P. simonii*, *S. psammophila*, *C. korshinskii* and *A. ordosica*) to identify their root distributions. We first dug the roots of each species in the locations where only single plants grow to identify their root characteristics (e.g., size, color, odor, orientation, etc) which we later used to distinguish species in mixed plots. The roots of *A. ordosica* have a pungent odor and those of *S. psammophila* are dark-red. The roots of *P. simonii* and *C. korshinskii* are yellow–brown, while the former is hard and has many branches. The latter is more flexible, and has relatively a few branches.

We then selected a sampling plot where all four plants coexist. At 0.5 m from the center of the plot, we established three soil cuboids that were 200 cm long (closest to the sampling plant), 140 cm deep, and 120 cm wide (Fig. 1d, e). Specifically, these three soil cuboids are at 120° angles to each other, forming a triangle around the center point. Each cuboid was excavated at 20-cm intervals for a depth interval of 0–140 cm. Then, the fine roots of all four species at each 20-cm depth interval were

Table 1
Morphological parameters (mean ± 1 s.d.) of the four plant species measured in the ecological sample survey.

	P. simonii	*C. korshinskii*	*S. psammophila*	*A. ordosica*
Growth form	Tree	Shrub	Shrub	Semi-shrub
Family	Salicaceae	Leguminosae	Salicaceae	Compositae
Leaf phenology	Deciduous	Deciduous	Deciduous	Deciduous
Average height in plots (m)	5.2 ± 1.6	1.4 ± 0.4	1.4 ± 0.4	0.5 ± 0.2
Average height of sampled plants (m)	5.2 ± 0.8	1.3 ± 0.4	1.4 ± 0.4	0.6 ± 0.3
Average basal diameter in plots (cm)	9.1 ± 5.9	1.6 ± 0.6	1.8 ± 0.5	0.8 ± 0.7
Average basal diameter of sampled plants (cm)	9.5 ± 1.0	1.5 ± 0.5	1.7 ± 0.5	0.9 ± 0.7
Density (individuals/ha)	519	494	301	3356
Root density (shallow layer, g/m^{-3})	247.7	45.0	102.9	54.0
Root density (intermediate layer, g/m^{-3})	144.0	42.3	50.0	29.2
Root density (deep layer, g/m^{-3})	45.4	12.4	8.1	3.2
Number of plants in plots	187	64	39	435

collected. These fine-root samples were rinsed, dried to constant masses at 60℃ for 24 h and fine-root mass of each plant species was determined in each depth interval.

2.5. Collections and measurements of water and leaf isotopes

Three fixed sites within the plot were selected to collect samples of xylem and soil water once a month from May to September in each of years 2018 and 2019. At each site, two mature plants for each species similar to the mean height and basal diameter of the species measured in the ecological sample survey were selected to collect xylem samples. Bark and phloem were peeled from fully suberized branches to avoid perturbance of xylem water isotopic composition by fractionation. Pieces of the de-barked and de-leaved twigs, 30 mm long, were then immediately placed in 10-mL vials. The vials were then sealed with caps and wrapped in Parafilm. These samples were kept in a cool box until storage in the lab at − 20℃.

Three soil profiles were collected simultaneously with the xylem samples in a randomized direction 100 cm from the center of sampled plants using a soil auger (diameter in 45 mm). Soil samples for each profile were obtained at 20 depths (at 10-cm intervals for a depth interval of 0–100 cm and at 20-cm intervals for a depth interval of 100–300 cm). The samples from each layer were separated into two parts: one part was used for determining gravimetric soil water content (SWC) using the oven-drying method (105℃ for 12 h); the other part was used for isotopic determination. Soil samples for isotopic determination were immediately placed in 10-mL vials that were sealed in the same manner as the xylem samples. In addition, we collected disturbed soil samples at 0–300 cm depths in the same depth interval as the soil isotope samples using a soil auger for determination of particle size using a MS 2000 Laser Particle Size Analyzer (Malvern Instruments, Malvern, UK).

We collected approximately 250 g of fresh leaves from branches of four plants of each species on the south-facing part of the crown monthly from May to September in each of years 2018 and 2019. The leaf samples were rinsed, dried to a constant mass at 60℃ for 72 h, and then ground to fine a powder that would pass through a 180-μm mesh sieve (#80). The samples were analyzed for $\delta^{13}C$ with a stable isotope ratio mass spectrometer (Isoprime 100, Isoprime Limited Inc., Cheadle, UK) that has a precision analysis of 0.1 ‰. $\delta^{13}C$ indicates the content of ^{13}C in a leaf sample relative to the Pee Dee Belemnite standard using standard per mil (‰) notation.

The δ^2H and $\delta^{18}O$ isotopic compositions of soil water from various depths (N = 60 for each month) and xylem water (N = 6 for each species each month) were determined with a stable isotope ratio mass spectrometer (Isoprime 100, Isoprime Limited Inc., Cheadle, UK). The precision of the analyses of H and O isotopes was 0.5 ‰ and 0.1 ‰, respectively. All H and O isotope ratios are expressed relative to Vienna Standard Mean Ocean Water (V-SMOW) using standard per mil (‰) notation. Prior to analysis, water was extracted from the soil and xylem (twig) samples with a LI-2100 automated vacuum distillation system (LICA Inc., Beijing, China), which is similar to cryogenic vacuum distillation systems except that it uses a compressor refrigeration unit and not liquid nitrogen (Dai et al., 2020; Zhao et al., 2021; Zhao and Wang, 2023). The extraction required 180 min with a maximum allowed vacuum pressure of 1500 Pa. Soil and xylem samples were weighed immediately prior to (M_{prior}) and after extraction (M_{post}). They were again weighed after oven drying at 105℃ for 12 h (M_{oven}) to calculate the water recovery efficiency of each sample ($\frac{M_{prior}-M_{oven}}{M_{prior}-M_{post}} \times 100\%$). The mean water recovery efficiency was more than 99 % for all samples.

2.6. Measurements of midday leaf water potential

Midday leaf water potential (ψ_{md}) for four plant species (N = 5 for each species each month) was determined once a month for May–September 2018–2019. Specifically, the ψ_{md} was measured between 12:30–13:30 using a Scholander-type pressure chamber (PMS 1000, PMS Instruments Inc., Corvalis, USA).

2.7. Calculation of WUEi

We derived WUEi from $\delta^{13}C$ measured in leaves of the four species based on the well-established theory linking leaf $\delta^{13}C$, isotopic carbon discrimination ($\Delta^{13}C$) and WUEi.

$$\Delta^{13}C = \frac{\delta^{13}C_a - \delta^{13}C_p}{1 + \delta^{13}C_p/1000} \quad (3)$$

where $\delta^{13}C_a$ and $\delta^{13}C_p$ are the $\delta^{13}C$ values of CO_2 in ambient air (assumed to be − 8 ‰; Seibt et al., 2008) and plant leaves, respectively.

$$WUE_i = \frac{C_a}{1.6}\frac{(b - \Delta^{13}C)}{(b - a)} \quad (4)$$

where a and b are isotopic fractionation coefficients (a = 4.4 ‰, fractionation during CO_2 diffusion through stomata; b = 27 ‰, fractionation associated with reactions by Rubisco and phosphoenol pyruvate-carboxylase; Schultz and Stoll, 2010). C_a is ambient CO_2 concentration. The C_a data was obtained from the Scripps Institution of Oceanography, San Diego (Keeling et al., 2001; https://scrippsco2.ucsd.edu/data/atmospheric_co2/spo.html).

2.8. Quantification of HNS based on xylem water δ^2H and $\delta^{18}O$ values

We used xylem water δ^2H and $\delta^{18}O$ values as input to the nicheROVER package to determine HNS. nicheROVER is a probabilistic method for determining niche region and pairwise niche overlaps (Swanson et al., 2015). The program produces a pairwise probability that the niche of one species overlaps with that of another (Swanson et al., 2015). nicheROVER calculates the extent of overlap between two species using niche regions (N_R), which are defined as specific locations where a species has a 95 % probability of being found. Uncertainty in overlap estimates was calculated using a Bayesian framework (Jackson et al.,

2011; Swanson et al., 2015). This overlap is bidirectional but asymmetric. The niche overlap of species A onto species B is determined as the fraction of the intersection area between niche A and niche B over the total niche area of B, and vice versa for species B. The higher the overlap, the lower the HNS. The original application presented by Swanson et al. (2015) used three-dimensional isotope data. In our application of nicheROVER we substitute species locations with locations where plants access water in three-dimensional space in the soil profile, based on isotopic signatures.

2.9. Determining the sources of plant water

We used the hierarchical cluster analysis based on between-groups linkage method to classify potential soil water sources. The measurement and transform method of the input data were set to "Squared Euclidean distance" and "Z-score", respectively. We identified three distinct soil layers (0–30 cm, 30–70 cm and 70–300 cm) based on similarities in $\delta^{18}O$ values in 2018–2019 as well as consideration of inter-month variability (see discussion in Fig. S2). We then quantified the relative contributions of potential water sources for the four plant species based on $\delta^{18}O$ and $\delta^{2}H$ values using the simmr package in R (Parnell et al., 2013). The model is fitted with a Monte Carlo Markov Chain algorithm that produces plausible solutions for each source's contribution to the content of xylem water in each sample. The mean and standard deviation of each source isotopic composition ($\delta^{2}H$ and $\delta^{18}O$) and xylem water composition were input into the model. The simmr package also incorporates uncertainty in trophic enrichment factors into the likelihoods of source contributions. As there is no isotope fractionation during root water uptake, the trophic enrichment factors were set to zero (Evaristo et al., 2016, 2017).

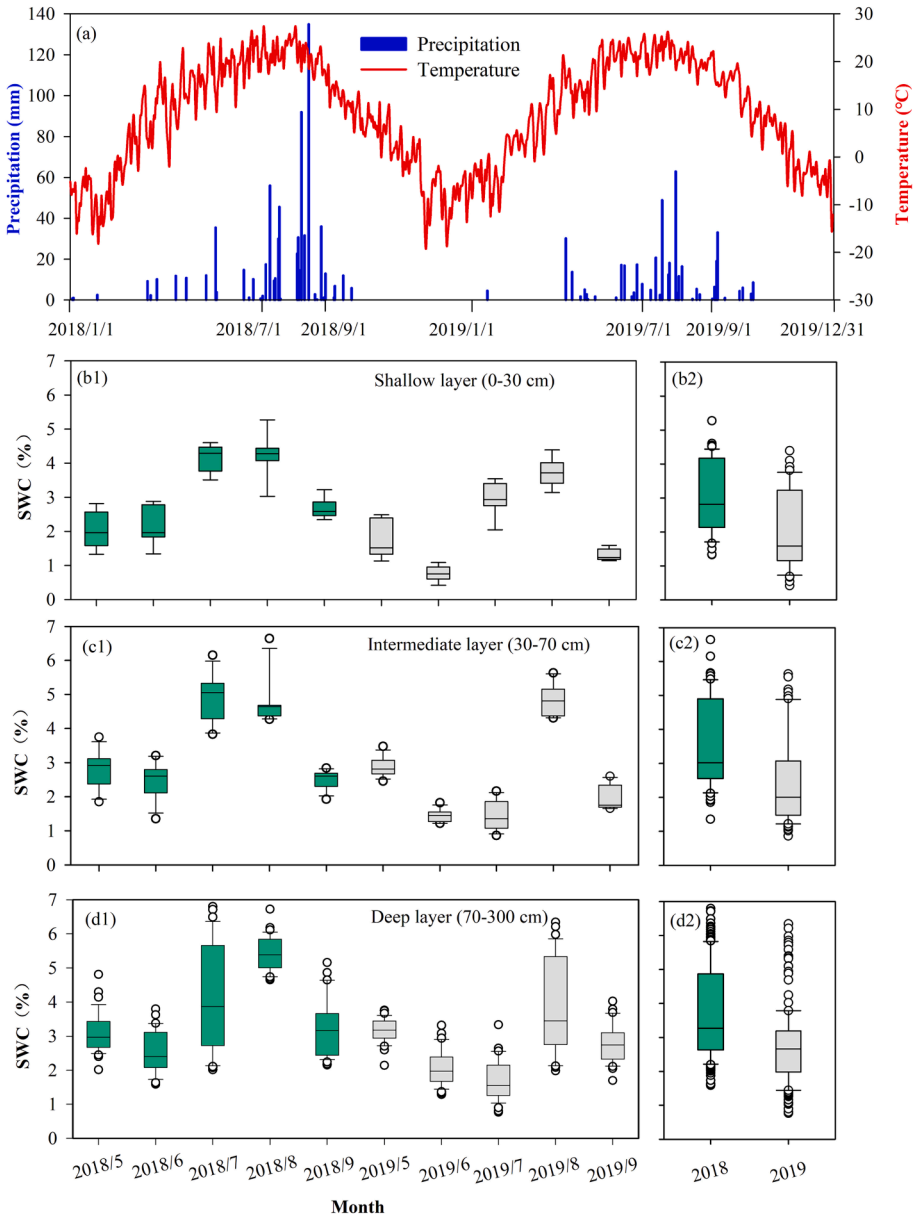

Fig. 2. Daily time series of precipitation and temperature (a), and boxplots of monthly and yearly variations in gravimetric soil water content (SWC) at shallow layer (b1–2, N = 9 per month), intermediate layer (c1–2, N = 12 per month) and deep layer (d1–2, N = 39 per month) for 2018 in green and 2019 in brown. Boxplots show the median (horizontal line), first to third quartiles (box), maximum and minimum values (whiskers) and outliers (points). (For interpretation of the references to color in this figure legend, the reader is referred to the web version of this article.)

2.10. Data analysis

Significant differences ($p < 0.05$) in water sources at different soil layers, WUEi and ψ_{md} among the four coexisting plant species in both wet and dry years, as well as the yearly variations of the above indicators for each species were identified using the bootstrap package in R (Efron and Tibshirani, 1994). The method employed herein does not require assumptions (e.g., normal distributions, equal variances), and provides robust results in many conditions that allow it to stand as a reliable alternative to standard parametric, nonparametric, and permutation tests in small sample size studies (Dwivedi et al., 2017; Hesterberg, 2011).

3. Results

3.1. Meteorological conditions

Precipitation during the two years of study was 708 mm (2018) and 424 mm (2019), representing a relatively wet year followed by a relatively dry year. During the experimentation periods (May–September of both years), the seasonal distribution of precipitation was uneven, mostly concentrated in July–August: 540 mm (76 %) in 2018; 220 mm (52 %) in 2019 (Fig. 2a). The mean temperature ranged from 16.7 °C in May to 22.3 °C in July during the two study years, combined. In response to variable precipitation depths, the gravimetric soil water contents (SWC) showed seasonal and yearly variation (Fig. 2b1, c1, d1). The mean SWC values of the shallow, intermediate, and deep layers in the relatively wet year of 2018 (3.1 %, 3.6 % and 3.7 %, respectively) were higher than in the relatively dry year of 2019 (2.1 %, 2.5 % and 2.7 %, respectively, Fig. 2b2, c2, d2).

3.2. Root distributions

The total fine-root mass of *P. simonii* (344.3 g, the mean from the three cubes) in the 3.36 m^3 sampling cube was much larger than the masses of the other three species: *C. korshinskii* (86.1 g), *S. psammophila* (113.0 g) and *A. ordosica* (60.1 g). The proportion of cumulative fine-root masses within 0–80 cm soil layer for *P. simonii*, *C. korshinskii*, *S. psammophila*, and *A. ordosica* accounted for 83 %, 83 %, 94 %, 97 %, respectively, of the total fine-root mass (Fig. 3). The differences in fine-root mass and distribution of fine-root in soil layers imply the various plants utilize somewhat different water sources.

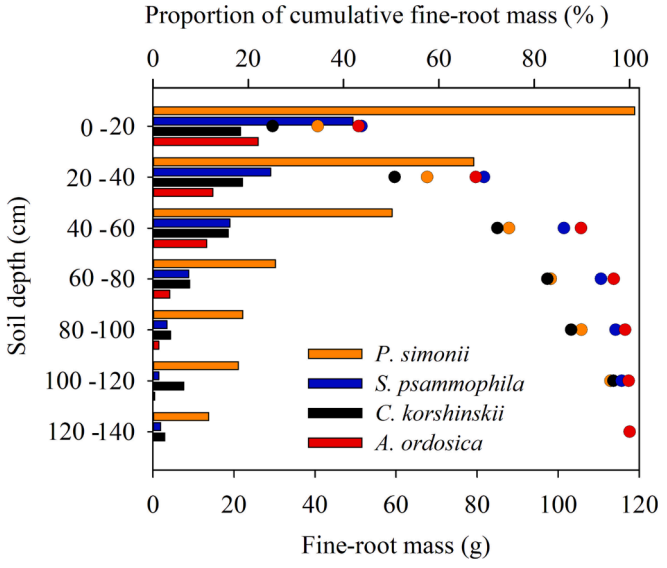

Fig. 3. Distributions of fine-root mass (bar) and the proportion of cumulative fine-root masses (scatter point) of *P. simonii*, *C. korshinskii*, *S. psammophila* and *A. ordosica*.

3.3. Water sources and physiological characteristics

The simmr model results indicate the following (Fig. 4a) for the May to September period of the relatively wet year (2018): (a) the dwarf tree *P. simonii* mainly used water from the deep layer (70–300 cm; mean of 41 %), with less utilized from the shallow (0–30 cm; 24 %) and intermediate (30–70 cm; 35 %) layers; (b) the shrub *C. korshinskii* used more water from the deep layer (39 %) and similar fractions of shallow soil water (30 %) and intermediate soil water (31 %); (c) the shrub *S. psammophila* used more water from the intermediate layer (38 %) and similar fractions of shallow soil water (33 %) and deep soil water (29 %); and (d) the semi-shrub *A. ordosica* generally relied mostly on shallow soil water (57 %), with limited use of water from the intermediate (24 %) and deep (19 %) layers.

The proportions of water use from shallow soil water by *P. simonii*, *C. korshinskii* and *S. psammophila* were significantly lower than that of *A. ordosica*; and *P. simonii* had a significantly higher fraction of water use from deep soil water (bootstrapping test). During the relatively dry year (2019), the proportions of water use from deep soil water increased to 54 %, 54 %, 53 % and 37 % for *P. simonii*, *C. korshinskii*, *S. psammophila* and *A. ordosica*, respectively (Fig. 4a). The increases of *S. psammophila* and *A. ordosica* were significant (bootstrapping test).

The ranges of ψ_{md} values for the four species were quite different and

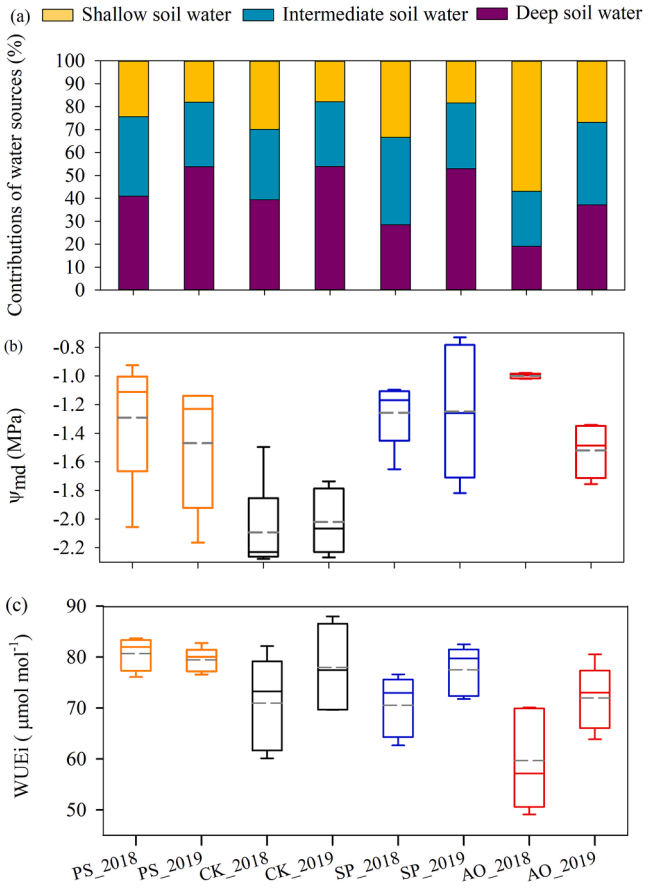

Fig. 4. Contributions of potential water sources (a), boxplots of midday leaf water potential (ψ_{md}, b) and intrinsic water use efficiency (WUEi, c) for PS (*P. simonii*), CK (*C. korshinskii*), SP (*S. psammophila*) and AO (*A. ordosica*) in the wet (2018) and dry (2019) years. Boxplots show the median (horizontal solid line), mean (horizontal grey dash line), first to third quartiles (box), maximum and minimum values (whiskers). Data was collected monthly from May to September 2018–2019 (N = 5 for each boxplot).

demonstrated yearly variability for *A. ordosica* (Fig. 4b). For example, ψ_{md} for *A. ordosica* significantly decreased (bootstrapping test) from the relatively wet year to the relatively dry year, but there was no significant change (bootstrapping test) in ψ_{md} of the other three species. Regarding inter-species differences, *C. korshinskii* showed consistently lower ψ_{md} (minimum value of − 2.3 MPa) than the other three species in both years (bootstrapping test). In fact, it was the only species where the median ψ_{md} was higher in the dry year than the wet year, although this response was not significant.

WUEi for *C. korshinskii*, *S. psammophila* and *A. ordosica*, increased significantly from the relatively wet year to the relatively dry year, whereas that for *P. simonii* generally remained stable (bootstrapping test, Fig. 4c). *A. orodosia* showed consistently lower WUEi than the other three species; WUEi for *C. korshinskii* and *S. psammophila* were intermediate; and WUEi for *P. simonii* was the highest recorded among the four species in both years (bootstrapping test). These patterns imply differentiation of physiological characteristics related to water use strategies between species.

3.4. Hydrological niche segregation

Based on the nicheROVER simulations, we find that in the relatively wet year (Fig. 5) *A. ordosica* water use was not occurring from the niche regions of *P. simonii* (6 % probability), *C. korshinskii* (7 %), and *S. psammophila* (22 %). These three species also had a relatively low probability of being found in the niche region of *A. ordosica*, suggesting HNS occurred between *A. ordosica* and the other three species. We also find an asymmetric overlap in isotope distributions between *P. simonii* and *C. korshinskii*, and between *P. simonii* and *S. psammophila*. *P. simonii* had a high probability of utilizing water in niche regions of *C. korshinskii* and *S. psammophila* (91 % and 95 %, respectively), while *C. korshinskii* and *S. psammophila* had low probabilities of water use from the *P. simonii* niche region (74 % and 67 %, respectively). The probabilities of *S. psammophila* and *C. korshinskii* using water from each other's niche regions were also high: 73 % (*S. psammophila* in *C. korshinskii*'s niche region); and 78 % (*C. korshinskii* in *S. psammophila*'s niche region).

In the relatively dry year, the trends of HNS between species were consistent with those in the wet year but the degree of segregation reduced slightly (Fig. 6). *A. ordosica* individuals still had the lowest probability of water usage from the niche regions of *P. simonii* (49 %),

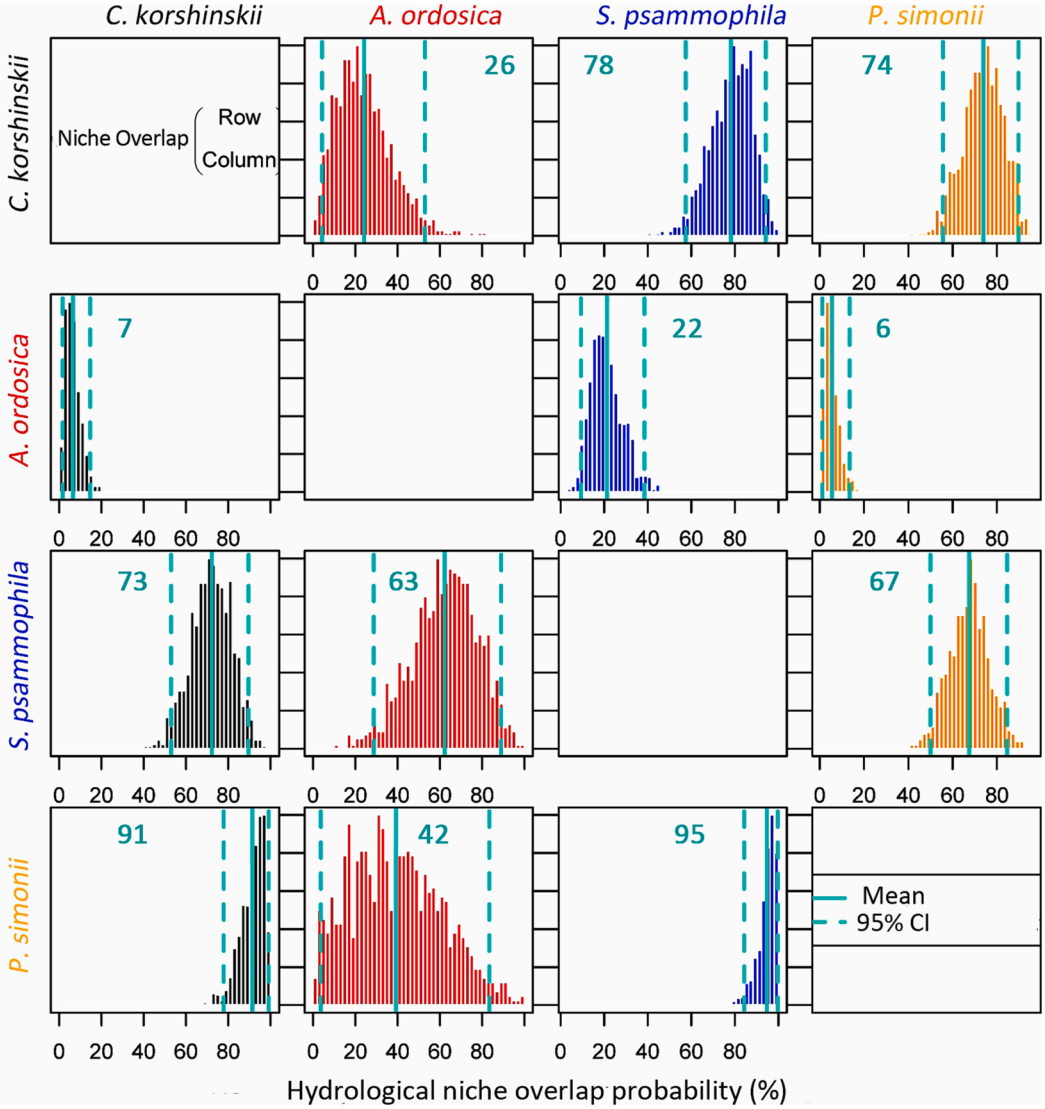

Fig. 5. Posterior distribution of the probabilistic niche overlap metric (%) for a specified N_R of 95% in 2018. The posterior means and 95% credible intervals are displayed in green. The numbers in the plots indicate the mean probability that an individual from the species indicated by row will be found within the niche of the species indicated by the column header. (For interpretation of the references to color in this figure legend, the reader is referred to the web version of this article.)

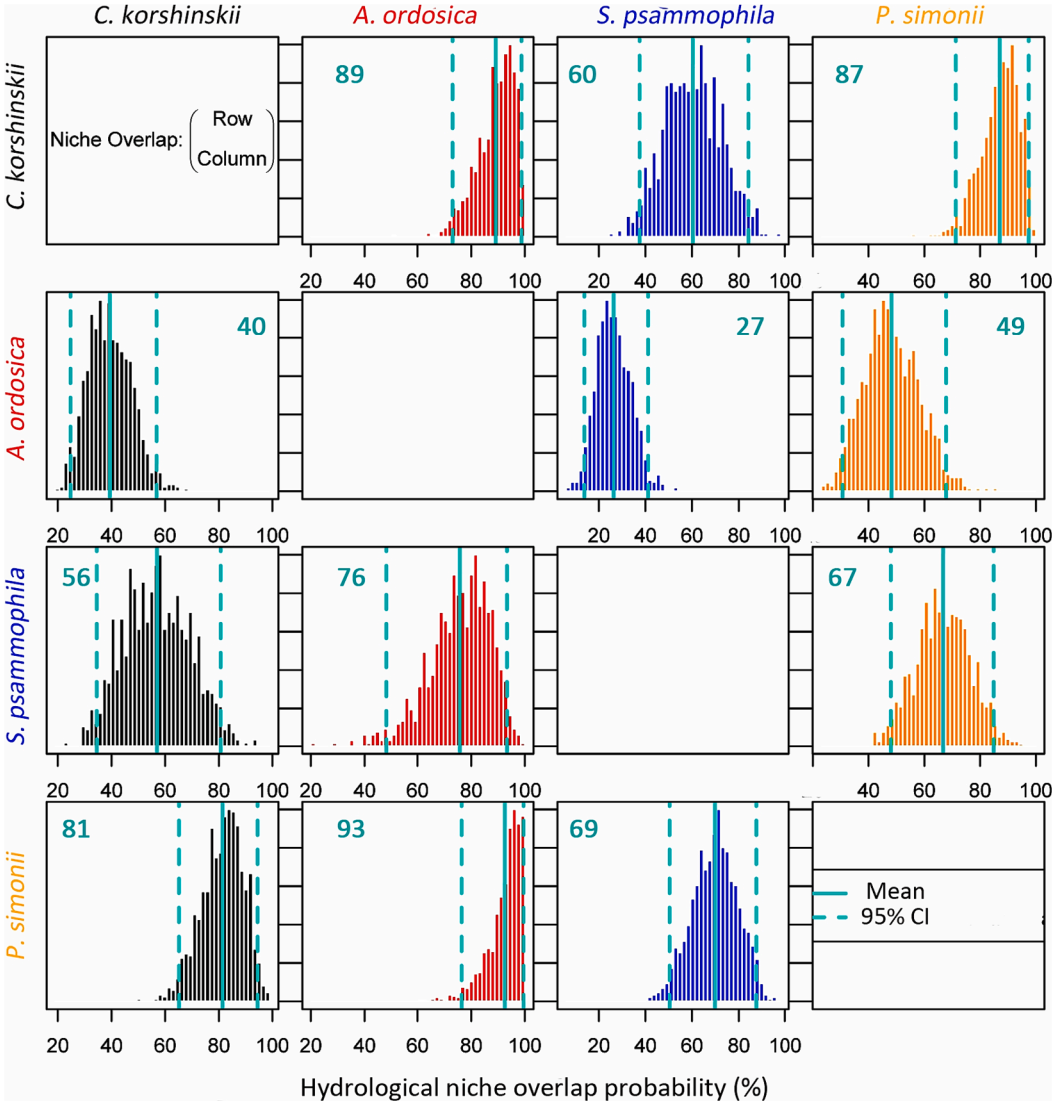

Fig. 6. Posterior distribution of the probabilistic niche overlap metric (%) for a specified N_R of 95% in 2019. The posterior means and 95% credible intervals are displayed in green. The numbers in the plots indicate the mean probability that an individual from the species indicated by row will be found within the niche of the species indicated by the column header. (For interpretation of the references to color in this figure legend, the reader is referred to the web version of this article.)

C. korshinskii (40 %), and *S. psammophila* (27 %). The probabilities of *P. simonii* and *C. korshinskii* using water from each other's niche regions were both more than 80 %. Meanwhile, the probability of overlap between *C. korshinskii* and *S. psammophila*, as well as *P. simonii* and *S. psammophila*, contracted to 60 % and 69 %, respectively.

4. Discussion

4.1. Water use strategies and hydrological niche segregation

The four plants exhibited diverse strategies to access various sources of water within the soil, resulting in distinct water use strategies (based on WUEi) and different degrees of HNS between the species across the two years having variable soil wetness (Fig. 7). At one end of the spectrum, the semi-shrub *A. ordosica* had few fine roots deeper than 100 cm and therefore tended to use water from the shallow soil in the relatively wet year. Conversely, the dwarf tree *P. simonii* relied consistently on deep soil water in both wet and dry years, optimizing high WUEi and keeping ψ_{md} stable—a result that is intuitive for a drought-tolerant species in an environment that dries from the surface downward. The root distribution data and the simmr model outputs also indicate that *P. simonii* extracted proportionally more water from the deeper layers than the shallow layers in both wet and dry years, likely in association with the presence of its fine-root masses at depth. In support, we observed a higher mass and greater proportion of fine roots in the deep layer for *P. simonii* compared with the other three species.

In the case of the shrubs, *C. korshinskii* relied on relatively deep soil water, while the other (*S. psammophila*) relied on intermediate soil water in the wet year, findings that agree with the root data showing that the proportion of fine roots at 80–140 cm in the soil layer for *C. korshinskii* (17 %) is higher than that for *S. psammophila* (6 %). While both improved WUEi in the relatively dry year by accessing relatively deeper water than in the wetter year, their responses in ψ_{md} were different. The ψ_{md} of *C. korshinskii* was significantly lower, indicating that *S. psammophila* may have stricter stomatal control compared with *C. korshinskii*. This characteristic is in line with data reported by Zhao et al. (2021) regarding looser stomatal regulation and lower ψ_{md} in *C. korshinskii* than in *S. psammophila*.

In prior work, Liu et al. (2010) reported that *S. psammophila* roots obtained soil water from an area about three times larger than its canopy radius. This "extended" horizontal range of the root system may increase *S. psammophila*' uptake of shallow and intermediate soil water, resulting

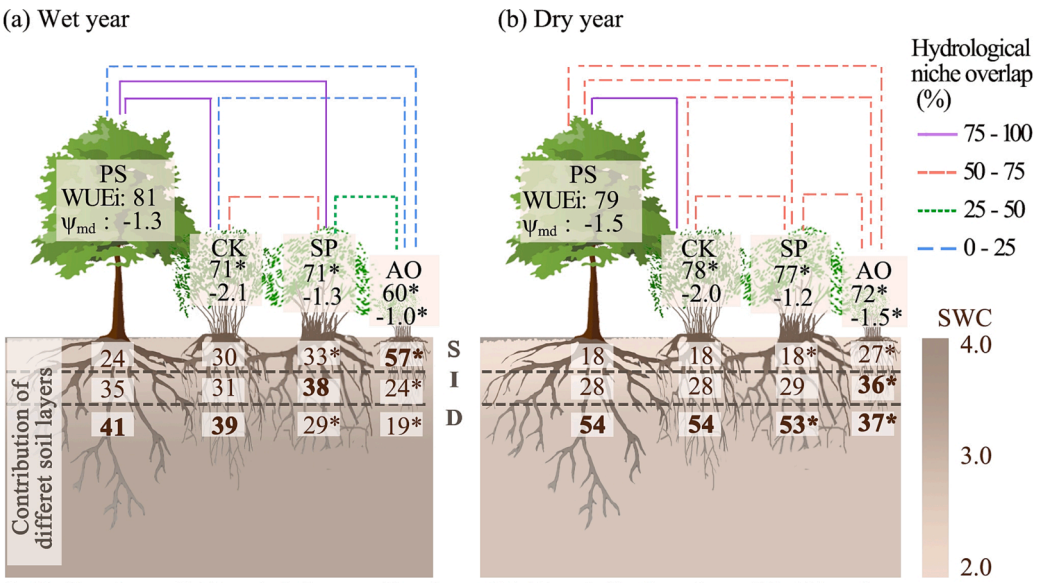

Fig. 7. Graphical summary of yearly changes in contributions of different soil layers, intrinsic water use efficiency (WUEi), midday leaf water potential (ψ_{md}), and hydrological niche overlap of the four coexisting species. Asterisks indicate significant differences in water source, WUEi and ψ_{md} for each species between the wet and the dry years. Hydrological niche overlap is the mean of species A versus species B and B versus A. The bold text in the soil profile indicates the water source that the species mainly relies on.

in distinct water sources between *S. psammophila* and the other two species in certain months (e.g., May–June in 2018, May in 2019, Fig. S3), and therefore greater HNS. We must keep in mind that our limited sampling of root masses may not accurately describe the root distribution of all species in the entire plot from which water is accessed.

Compared with the other three species, *A. orodosia* had the lowest WUEi, probably because of its inability to access deep soil water owing to limited root distribution. We found a "moderate" but negative correlation between the contribution of shallow soil water and WUEi ($R^2 = 0.37$, $p < 0.001$; Fig. S4a), as well as a similarly moderate positive correlation between the contribution of deep soil water and WUEi ($R^2 = 0.38$, $p < 0.001$; Fig. S4c). Unfortunately, our limited number of samples does not allow us to explore this relationship in more detail for individual species.

Notably, the magnitude of the observed HNS varied with water availability. The hydrological niche of *A. ordosica* was clearly separated from those of the other three species in the wetter year when there was a very low probability (6–22 %) of it using water from the hydrological niches of the other species. However, that probability expanded to 27–49 % in the relatively dry year, reducing the degree of segregation.

Similar trends were observed in the Taihang Mountains of China, where *Vitex negundo* L. var. heterophylla had a high hydrological niche overlap with *Robinia pseudoacacia* L and *Ziziphus jujuba* Mill var. spinosa during the dry season (Zhu et al., 2021). Also similar to our findings, HNS at the Taihang site expanded in the rainy season. Elsewhere, dynamic HNS might have played a significant role in drought-driven changes in vegetation productivity, composition and structure that have been demonstrated in tropical forests of Mexico (Rodríguez-Robles et al., 2020), seasonal tropical forests of Brazil (Brum et al., 2019), and gypsum hill of NE Spain (Palacio et al., 2017), as well as Sagebrush steppe of US (Kulmatiski et al., 2020b). Exploring HNS dynamics has become even more important with observed changes in climate variability and warming. The projected increases in drought frequency and intensity in some regions may alter the specific frequency in patterns of water availability, as well as plant co-associations, for which certain species have evolved or adapted to cope with water stress (Chitra-Tarak et al., 2018).

Collectively, the observed decrease in the degree of HNS in the relatively dry year indicates an increase in competition for water among the plant species, which is plausible for plants competing for scarce water in a semi-arid ecosystem. Again, the strategy for all species was to rely more heavily on deeper soil water sources in the relatively dry year, but to different degrees (Fig. 7). Consequently, these shifts in water source usage and changes in the probabilities of hydrological niche overlap from the wet year to the dry year indicate that HNS is dynamic on at least an annual time scale in response to fluctuating soil moisture patterns, supporting one of our original hypotheses.

4.2. Broader implications with hydrological niche segregation and $\delta^{13}C$

Over a 2-year period, we examined how four coexisting plant species used water in a semi-arid ecosystem. We have shown that, niche segregation in rooting patterns of the four plant species resulted in diverse root water uptake profiles. Notably, hydrological niches change throughout the year as they adjust water use based on soil water availability. These results show the degree to which a plant's hydrological niche varies in response to changes in soil moisture and competition with other plants. This finding could have implications for plant restoration and conservation practices, especially against the backdrop of hydrologic uncertainty related to climate change.

The finding that different species dynamically segregate the hydrological niche by changing their water uptake depths could be broadly significant, as (a) both changing temperature and precipitation are likely to alter hydrological conditions variably at fine scales and (b) changes in root water uptake strategies in response to changing soil moisture levels are generally the case, with spatio-temporal variations, perhaps, because of species (Zhao and Wang, 2018) and phylogenetic underpinnings (Knighton et al., 2021). Current niche-based bioclimatic models that project plant species response to climate change do not account for hydrological niche changing with soil moisture fluctuations at finer

scales (Midgley et al., 2003). Our study provides empirical basis for understanding how plants compete for water within the framework of hydrological niche segregation.

During the study, the leaf $\delta^{13}C$ values ranged from − 29.0 ‰ to − 27.3 ‰ for the four coexisting plant species. In semi-arid regions similar to our study's setting, leaf $\delta^{13}C$ values have also displayed considerable variation among plant species. For peach, walnut, and apple trees, the values have ranged from − 26.4 ‰ to − 28.7 ‰, as reported by Wu et al., (2022b). Similarly, *Robinia pseudoacacia*, *Armeniaca sibirica* and *Ailanthus altissima* have shown a range between − 26.3 ‰ and − 28.0 ‰ (Wang et al., 2020). Even within the same species, variations in leaf $\delta^{13}C$ values for *C. korshinskii* across eight different sites in CLP and Qinling Mountain have shown a range between − 27.0 ‰ and − 23.3 ‰ (Zheng and Shangguan, 2007).

The observed wide variations in leaf $\delta^{13}C$ values, both interspecifically and intra-specifically, suggest that plants exhibit specific adjustments in response to changing soil moisture conditions and water competition. Our study points to the interplay between these variable leaf $\delta^{13}C$ values, water sources, and hydrological niches. This understanding offers insights into the coordination between water use strategies related to the contribution of deep soil water and WUEi. Understanding these natural variations in leaf $\delta^{13}C$ values is crucial for evaluating how individual plants adapt to drought conditions.

4.3. Methodology considerations and limitations

Of the two methods we used to assess the water competition between species on the CLP, one quantifies the contributions of potential water sources through comparisons of isotopes in the xylem water and the water within the soil profile (simmr model); the other quantifies the probability of hydrological niche overlap based on isotopic compositions of xylem water of the four species alone (nicheROVER model). The results regarding water source access by the two methods were generally consistent, but with one exception. In agreement, two pairs of species (*S. psammophila* and *C. korshinskii*) and (*S. psammophila* and *P. simonii*) exhibited higher HNS in the dry year, but the two methods indicated differences regarding where they accessed water. The difference may be related to *P. simonii* and *C. korshinskii* having a lower proportion of roots available at the depth of 0–60 cm (75 % and 72 %, respectively) than *S. psammophila* (86 %, Fig. 3). Here, we acknowledge that the lack of data on water use volume hinders us from further exploring which method is closer to the real situation. In any case, both methods indicate that hydrological niches are dynamic, supporting the main finding in the study.

Our research adds to the understanding of dynamic HNS based on consideration of stable isotope signatures. However, while the results are plausible, we cannot confidently say that combining stable isotope tracers with the nicheROVER model fully captures the extent of hydrological niches. Further, we could not determine with certainty the response of the four coexisting plant species to prolonged dry conditions because the relatively dry year when we collected our samples followed a relatively wet year. More data from a variety of wetness conditions and other species might have better illuminated a broader hydrological niche.

Further, we note two limitations to our approach in classifying 'wet' and 'dry' years. Firstly, the use of '0.33' as a multiplier in expressions (1) and (2) may not be universally applicable across different climatic regions. Secondly, these expressions assume a normal distribution of precipitation data, which is rarely the case. Thus, while these empirical expressions, developed by earlier researchers offer a straightforward approach to classifying precipitation years, they may require adjustments or supplementary methods for more accurate and robust analysis.

Finally, we only considered water as a limiting factor on community structure, but we recognize that light and nutrient availability also play important roles in vegetation dynamics (Brum et al., 2019; Stark et al., 2012, 2015). Future research should focus on quantifying the potential trade-offs between plant water uptake and light availability at the community level and modeling water dynamics at the rhizosphere scale (Daly et al., 2017).

5. Conclusion

Our two-year study in a dry ecosystem illuminated the dynamic nature of water utilization among four coexisting plant species. We found that the four coexisting plant species in this semi-arid ecosystem (*P. simonii*, *C. korshinskii*, *S. psammophila* and *A. ordosica*) segregate along a hydrological niche axis characterized by distinct water sources, exhibiting varying water use efficiencies (WUEi) that largely align with root architecture and vegetation form (tree, shrub, semi-shrub). Particularly noteworthy is the dynamic nature of the hydrological niches, which contracted during a relatively dry year due to shifts toward greater utilization of deep soil water sources. The shrub and semi-shrub species (*C. korshinskii*, *S. psammophila* and *A. ordosica*) increased their use of deep soil water and concurrently improved WUEi during the relatively dry year. In contrast, the dwarf tree *P. simonii* consistently accessed deeper soil layers for water across both wet and dry years, with its WUEi remaining relatively unchanged. This adaptive response by some plants to variable environmental conditions holds global significance, given the non-uniform distribution of precipitation worldwide and likelihood that many plants adjust their water use strategies in response to soil moisture levels. Our research underscores the fluidity of HNS among coexisting plant species in semi-arid ecosystems, reflecting their capacity to adapt water resource acquisition strategies in response to varying soil moisture levels. Understanding these dynamics provides valuable insights into predicting future alterations in the composition and structure of plant communities within dry regions, considering climate variability and anticipated climate changes.

CRediT authorship contribution statement

Ying Zhao: Conceptualization, Investigation, Methodology, Writing – original draft, Writing – review & editing, Software, Visualization. **Li Wang:** Conceptualization, Funding acquisition, Methodology, Resources, Supervision, Writing – original draft, Writing – review & editing, Validation, Visualization. **Kwok P. Chun:** Supervision, Validation, Writing – review & editing, Methodology, Visualization. **Alan D. Ziegler:** Methodology, Supervision, Writing – original draft, Writing – review & editing, Data curation, Validation, Visualization. **Jaivime Evaristo:** Conceptualization, Methodology, Resources, Supervision, Validation, Visualization, Writing – original draft, Writing – review & editing, Data curation, Formal analysis.

Declaration of competing interest

The authors declare that they have no known competing financial interests or personal relationships that could have appeared to influence the work reported in this paper.

Data availability

Data on soil water, xylem water isotopes ($\delta^{2}H$, $\delta^{18}O$) and intrinsic water use efficiency of the four coexisting plant species in Supplementary material.

Acknowledgements

Jaivime Evaristo and Ying Zhao thank Prof. Martin Wassen and Prof. Stefan Dekker of the Copernicus Institute of Sustainable Development, Faculty of Geosciences, for making the research visit of Ying Zhao to Utrecht University possible. This work was supported by the National Natural Science Foundation of China (41977012; 42171043; 42377318), the Strategic Priority Research Program of Chinese

Academy of Sciences (XDB40000000) and the State Key Laboratory of Loess and Quaternary Geology, Institute of Earth Environment, CAS (SKLLQG1718).

Appendix A

Supplementary data to this article can be found online at https://doi.org/10.1016/j.jhydrol.2024.130677.

References

Angert, A.L., Huxman, T.E., Chesson, P., Venable, D.L., 2009. Functional tradeoffs determine species coexistence via the storage effect. Proc. Natl. Acad. Sci. U. S. A. 106, 11641–11645.

Araya, Y.N., Silvertown, J., Gowing, D.J., McConway, K., Linder, P., Midgley, G., 2010. Variation in $\delta^{13}C$ among species and sexes in the family Restionaceae along a fine-scale hydrological gradient. Austral Ecol. 35, 818–824.

Araya, Y.N., Silvertown, J., Gowing, D.J., McConway, K.J., Linder, H.P., Midgley, G., 2011. A fundamental, eco-hydrological basis for niche segregation in plant communities. New Phytol. 189, 253–258.

Bartelheimer, M., Gowing, D.J., Silvertown, J., 2010. Explaining hydrological niches: the decisive role of below-ground competition in two closely related Senecio species. J. Ecol. 98, 126–136.

Brum, M., Teodoro, G.S., Abrahão, A., Oliveira, R.S., 2017. Coordination of rooting depth and leaf hydraulic traits defines drought-related strategies in the campos rupestres, a tropical montane biodiversity hotspot. Plant Soil 420, 467–480.

Brum, M., Vadeboncoeur, M.A., Ivanov, V., Asbjornsen, H., Saleska, S., Alves, L.F., Penha, D., et al., 2019. Hydrological niche segregation defines forest structure and drought tolerance strategies in a seasonal Amazon forest. J. Ecol. 107, 318–333.

Brunner, I., Herzog, C., Dawes, M.A., Arend, M., Sperisen, C., 2015. How tree roots respond to drought. Front. Plant Sci. 6, 547.

Camarero, J.J., Sanchez-Salguero, R., Sanguesa-Sarreda, G., Matias, L., 2018. Tree species from contrasting hydrological niches show divergent growth and water-use efficiency. Dendrochronologia 52, 87–95.

Cao, S.X., 2008. Why large-scale afforestation efforts in China have failed to solve the desertification problem. Environ. Sci. Tech. 42 (6), 1826–1831.

Cao, S.X., Tian, T., Chen, L., Dong, X.B., Yu, X.X., Wang, G.S., 2010. Damage caused to the environment by reforestation policies in arid and semi-arid areas of China. Ambio 39, 279–283.

Cao, S.X., Chen, L., Shankman, D., Wang, C.M., Wang, X.B., Zhang, H., 2011. Excessive reliance on afforestation in China's arid and semi-arid regions: lessons in ecological restoration. Earth Sci. Rev. 104, 240–245.

Case, M.F., Nippert, J.B., Holdo, R.M., Staver, A.C., 2020. Root-niche separation between savanna trees and grasses is greater on sandier soils. J. Ecol. 00, 1–11.

Chen, Y., Wang, K., Lin, Y., Shi, W., Song, Y., He, X., 2015. Balancing green and grain trade. Nat. Geosci. 8, 739–741.

Chitra-Tarak, R., Ruiz, L., Dattaraja, H.S., Kumar, M.S.M., Riotte, J., Suresh, H.S., McMahon, S.M., et al., 2018. The roots of the drought: hydrology and water uptake strategies mediate forest-wide demographic response to precipitation. J. Ecol. 106, 1495–1507.

Dai, J.J., Zhang, X.P., Luo, Z.D., Wang, R., Liu, Z.L., He, X.G., Rao, Z.G., et al., 2020. Variation of the stable isotopes of water in the soil-plant-atmosphere continuum of a *Cinnamomum camphora* woodland in the East Asian monsoon region. J. Hydrol. 589, 125199.

Daly, K.R., Cooper, L.J., Koebernick, N., Evaristo, J., Keyes, S.D., van Veelen, A., Roose, T., 2017. Modelling water dynamics in the rhizosphere. Rhizosphere 4, 139–151.

Dwivedi, A.K., Mallawaarachchi, I., Alvarado, L.A., 2017. Analysis of small sample size studies using nonparametric bootstrap test with pooled resampling method. Stat. Med. 36 (14), 2187–2205.

Dwyer, C., Pakeman, R.J., Jones, L., van Willegen, L., Hunt, N., Millett, J., 2021. Fine-scale hydrological niche segregation in coastal dune slacks. J. Veg. Sci. 32, e13085.

Efron, B., Tibshirani, R.J., 1994. An introduction to the bootstrap. CRC Press.

Evaristo, J., McDonnell, J.J., Scholl, M.A., Bruijnzeel, L.A., Chun, K.P., 2016. Insights into plant water uptake from xylem-water isotope measurements in two tropical catchments with contrasting moisture conditions. Hydrol. Process. 30, 3210–3227.

Evaristo, J., McDonnell, J.J., Clemens, J., 2017. Plant source water apportionment using stable isotopes: a comparison of simple linear, two-compartment mixing model approaches. Hydrol. Process. 31, 3750–3758.

Fu, B.J., Wang, S., Liu, Y., Liu, J.B., Liang, W., Miaom, C.Y., 2017. Hydrogeomorphic ecosystem responses to natural and anthropogenic changes in the Loess Plateau of China. Annu. Rev. Earth Planet. Sci. 45, 223–243.

Granda, E., Antunes, C., Máguas, C., Castro-Díez, P., 2022. Water use partitioning of native and non-native tree species in riparian ecosystems under contrasting climatic conditions. Funct. Ecol. 36, 2480–2492.

Hesterberg, T., 2011. Bootstrap. Wiley Interdiscip. Rev. Comput. Stat. 3 (6), 497–526.

Holdo, R.M., Nippert, J.B., 2023. Linking resource- and disturbance- based models to explain tree-grass coexistence in savannas. New Phytol. 237, 1966–1979.

Illuminati, A., Querejeta, J.I., Pias, B., Escudero, A., Matesanz, S., 2022. Coordination between water uptake depth and the leaf economic spectrum in a Mediterranean shrubland. J. Ecol. 110, 1844–1856.

Ivanov, V.Y., Hutyra, L.R., Wofsy, S.C., Munger, J.W., Saleska, S.R., de Oliveira Jr, R.C., de Camargom, P.B., 2012. Root niche separation can explain avoidance of seasonal drought stress and vulnerability of overstory trees to extended drought in a mature Amazonian forest. Water Resour. Res. 48, W12507.

Jackson, A.L., Inger, R., Parnell, A.C., Bearhop, S., 2011. Comparing isotopic niche widths among and within communities: SIBER-Stable Isotope Bayesian Ellipses in R. J. Anim. Ecol. 80, 595–602.

Kang, Y.X., Kang, B.W., Yue, W.J., Liang, Z.S., Lei, R.D., 2007. The classification of *Quercus liaotungensis* communities and their nich in Loess Plateau of North Shaanxi. Acta Ecol. Sin. 27, 4096–4105 (in Chinese with English abstract).

Kang, J., Peng, Y.F., Xu, W.F., 2022. Crop root responses to drought stress: molecular mechanisms, nutrient regulations, and interactions with microorganisms in the rhizosphere. Int. J. Mol. Sci. 23 (16), 9310.

Keeling, C.D., Piper, S.C., Bacastoe, R.B., Wahlen, M., Whorf, T.P., Heimann, M., Meijer, H.A. 2001. Exchanges of atmospheric CO_2 and $^{13}CO_2$ with the terrestrial biosphere and oceans from 1978 to 2000. I. Global aspects, SIO Reference Series, No. 01-06, Scripps Institution of Oceanography, San Diego, 88.

Knighton, J., Fricke, E., Evaristo, J., de Boer, H.J., Wassen, M.J., 2021. Phylogenetic underpinning of groundwater use by trees. Geophys. Res. Lett. 48, e2021GL093858.

Kulmatiski, A., Adler, P.B., Foley, K.M., 2020a. Hydrologic niches explain species coexistence and abundance in a shrub-steppe system. J. Ecol. 108, 998–1008.

Kulmatiski, A., Beard, K.H., 2022. A modern two-layer hypothesis helps resolve the 'savanna problem'. Ecol. Lett. 25 (9), 1952–1960.

Kulmatiski, A., Beard, K.H., Holdrege, M.C., February, E.C., 2020b. Small differences in root distributions allow resource niche partitioning. Ecol. Evol. 10, 9776–9787.

Liu, T.S., 1985. Loess and the environment. (China's). Science Press, Beijing (in Chinese).

Liu, J., He, X., Bao, H.L., Zhou, C.J., 2010. Distribution of fine roots of *Salix psammophila* and its relationship with soil moisture in Mu Us sandland. J. Desert Res. 30 (6), 1362–1366 (in Chinese with English abstract).

Lu, F., Hu, H.F., Sun, W.J., Zhu, J.J., Liu, G.B., Zhou, W.M., Zhang, Q.F., et al., 2018. Effects of national ecological restoration projects on carbon sequestration in China from 2001 to 2010. Proc. Natl. Acad. Sci. U. S. A. 115 (16), 4039–4044.

Matos, I.S., Binks, O., Eller, C.B., Zorger, B.B., Meir, P., Dawson, T.E., Rosado, B.H., 2022. Revisiting plant hydrological niches: the importance of atmospheric resources for ground-rooted plants. J. Ecol. 110 (8), 1746–1756.

Midgley, G.F., Hannah, L., Millar, D., Thuiller, W., Booth, A., 2003. Developing regional and species-level assessments of climate change impacts on biodiversity in the cape floristic region. Biol. Conserv. 112, 87–97.

Miguez-Macho, G., Fan, Y., 2021. Spatiotemporal origin of soil water taken up by vegetation. Nature 598 (7882), 624–628.

Moreno-Gutierrez, C., Dawson, T.E., Nicolas, E., Querejeta, J.I., 2012. Isotopes reveal contrasting water use strategies among coexisting plant species in a Mediterranean ecosystem. New Phytol. 196 (2), 489–496.

Palacio, S., Montserrat-Marti, G., Ferrio, J.P., 2017. Water use segregation among plants with contrasting root depth and distribution along gypsum hills. J. Veg. Sci. 28, 1107–1117.

Parnell, A.C., Phillips, D.L., Bearhop, S., Semmens, B.X., Ward, E.J., Moore, J.W., Jackson, A.L., et al., 2013. Bayesian stable isotope mixing models. Environmetrics 24 (6), 387–399.

Rodríguez-Robles, U., Arredondo, J.T., Huber-Sannwald, E., Yepez, E.A., Ramos-Leal, J. A., 2020. Coupled plant traits adapted to wetting/drying cycles of substrates co-define niche multidimensionality. Plant Cell Environ. 43, 2394–2408.

Schultz, H.R., Stoll, M., 2010. Some critical issues in environmental physiology of grapevines: future challenges and current limitations. Aust. J. Grape Wine Res. 16, 4–24.

Seibt, U., Rajabi, A., Griffiths, H., Berry, J.A., 2008. Carbon isotopes and water use efficiency: sense and sensitivity. Oecologia 155 (3), 441–454.

Silvertown, J., Araya, Y., Gowing, D., 2015. Hydrological niches in terrestrial plant communities: a review. J. Ecol. 103, 93–108.

Stark, S.C., Leitold, V., Wu, J.L., Hunter, M.O., de Castilho, C.V., Costa, F.R.C., McMahon, S.M., et al., 2012. Amazon forest carbon dynamics predicted by profiles of canopy leaf area and light environment. Ecol. Lett. 15, 1406–1414.

Stark, S.C., Enquist, B.J., Saleska, S.R., Leitold, V., Schietti, J., Longo, M., Alves, L.F., et al., 2015. Linking canopy leaf area and light environments with tree size distributions to explain Amazon forest demography. Ecol. Lett. 18, 636–645.

Swanson, H., Lysy, M., Ehrman-Stasko, A., Johnson, J., Reist, J., 2015. A new probabilistic method for quantifying *n*-dimensional ecological niches and niche overlap. Ecology 96, 318–324.

Tao, L.W., Ma, H., Ge, F.L., 2000. Analysis on the characteristics of precipitation in Shanxi Province. Shanxi Meteorology 5, 6–9 (in Chinese).

Tsunekawa, A., Liu, G., Yamanaka, N., Du, S. (Eds.), 2014. Restoration and Development of the Degraded Loess Plateau. Springer Japan, Tokyo.

Walter, H., 1939. Grasland, Savanne und Busch der arideren Teile Afrikas in ihrer ökologischen Bedingtheit. Jahrb Wiss Bot 87, 750–860.

Wang, J., Fu, B.J., Wang, L.X., Lu, N., Li, J.Y., 2020. Water use characteristics of the common tree species in different plantation types in the Loess Plateau of China. Agric. For. Meteorol. 288–289, 108020.

Wang, S.Y., Wang, L., Han, X., Zhang, L.S., 2016. Evapotranspiration characteristics of apple orchard at peak period of fruiting in loess tableland. Scientia Silvae Sincae 52 (1), 128–135 (in Chinese with English abstract).

Ward, D., Wiegand, K., Getzin, S., 2013. Walter's two-layer hypothesis revisited: back to the roots! Oecologia 172, 617–630.

Wu, W.J., Tao, Z., Chen, G.J., Meng, T.F., Li, Y., Feng, H., Si, B.C., et al., 2022b. Phenology determines water use strategies of three economic tree species in the semi-arid Loess Plateau of China. Agric. For. Meteorol. 312, 108716.

Wu, J.E., Zeng, H.H., Zhao, F., Chen, C.F., Singh, A.K., Jiang, X.J., Yang, B., Liu, W.J., 2022a. Plant hydrological niches become narrow but stable as the complexity of interspecific competition increases. Agric. For. Meteorol. 320, 108953.

Yuan, C., Gao, G.Y., Fu, B.J., 2017. Comparisons of stemflow and its bio-abiotic influential factors between two xerophytic shrub species. Hydrol. Earth Syst. Sci. 21, 1421–1438.
Zhang, P.C., Wang, B.K., Tang, K.L., 1993. The environmental geomorphology characteristics of Shenmu experimental area. Memoir of NISWC, Academia Sinica and Ministry of Water Resources 18, 16–23 (in Chinese with English abstract).
Zhao, Y., Wang, L., 2018. Plant water use strategy in response to spatial and temporal variation in precipitation patterns in China: a stable isotope analysis. Forests 9, 123.
Zhao, Y., Wang, L., 2023. Coordination of available soil water content and root distribution modifies water source apportionment of the shrub plant *Caragana korshinskii*. Sci. Total Environ. 900, 165893.
Zhao, Y., Wang, L., Knighton, J., Evaristo, J., Wassen, M., 2021. Contrasting adaptive strategies by *Caragana korshinskii* and *Salix psammophila* in a semiarid revegetated ecosystem. Agric. For. Meteorol. 300, 108323.
Zhao, Y., Dai, J.J., Tang, Y.K., Wang, L., 2022. Illuminating isotopic offset between bulk soil water and xylem water under different soil water conditions. Agric. For. Meteorol. 325, 109150.
Zheng, S.X., Shangguan, Z.P., 2007. Spatial patterns of foliar stable carbon isotope compositions of C_3 plant species in the Loess Plateau of China. Ecol. Res. 22, 342–353.
Zhu, W.R., Li, W.H., Shi, P.L., Cao, J.S., Zong, N., Geng, S.B., 2021. Intensified interspecific competition for water after afforestation with *Robinia pseudoacacia* into a native shrubland in the Taihang Mountains. Northern China. Sustainability 13, 807.